



THE UNIVERSITY *of* EDINBURGH

Edinburgh Research Explorer

Two-stage Optimisation of Hybrid Solar Power Plants

Citation for published version:

Bravo, R & Friedrich, D 2018, 'Two-stage Optimisation of Hybrid Solar Power Plants', *Solar Energy*, vol. 164, pp. 187-199. <https://doi.org/10.1016/j.solener.2018.01.078>

Digital Object Identifier (DOI):

[10.1016/j.solener.2018.01.078](https://doi.org/10.1016/j.solener.2018.01.078)

Link:

[Link to publication record in Edinburgh Research Explorer](#)

Document Version:

Peer reviewed version

Published In:

Solar Energy

General rights

Copyright for the publications made accessible via the Edinburgh Research Explorer is retained by the author(s) and / or other copyright owners and it is a condition of accessing these publications that users recognise and abide by the legal requirements associated with these rights.

Take down policy

The University of Edinburgh has made every reasonable effort to ensure that Edinburgh Research Explorer content complies with UK legislation. If you believe that the public display of this file breaches copyright please contact openaccess@ed.ac.uk providing details, and we will remove access to the work immediately and investigate your claim.



Two-stage Optimisation of Hybrid Solar Power Plants

R.Bravo¹, D.Friedrich*

School of Engineering, Institute for Energy Systems, The University of Edinburgh, UK

Abstract

Hybrid solar power plants which combine concentrated solar power (CSP) and photovoltaic (PV) systems with thermal energy storage (TES) have the potential to provide cost competitive and dispatchable renewable energy. The integration of energy storage gives dispatchability to the variable renewable generation while the combination of different generation technologies can reduce the costs. However, the design of reliable and cost competitive hybrid solar power plants requires the careful balancing of trade-offs between financial and technical performance. This is made more complicated by the dependence on a larger number of parameters compared to conventional plants and due to the integration of TES which requires that the operational profile is optimised for every design. This contribution presents a two-stage, multi-objective optimisation framework which combines multi-objective linear programming methods for the operational optimisation with multi-objective genetic algorithms for the design optimisation. The operational optimisation which is performed for every design point needs to be performed with linear programming methods. Here an automated scalarisation method is developed for the linear programming method which enables the multi-objective optimisation of the operational profile. This enables the evaluation of the trade-offs between financial and technical performance in both the design and operational optimisation, which is required to design reliable and cost competitive sustainable energy systems. The two-stage multi-objective optimisation is applied to analyse and improve the design of the hybrid solar power plant Atacama-1. It is demonstrated that balancing the trade-off between financial and technical performance is key to increase the competitiveness of solar energy and that it is possible to simultaneously increase dispatchability and decrease the levelised cost of energy. This shows that the operational and design optimisations have to be directly linked in order to exploit the synergies of hybrid systems. Thus the optimisation framework presented in this study can improve the decision making in the design of hybrid solar power plants.

Keywords: Hybrid energy systems, Thermal energy storage, Linear programming, Two-stage, multi-objective optimisation

1. Introduction

During the last year, the new installed capacity of renewable energy projects in the power sector was greater than the development of conventional energy systems [1], and nowadays renewable energy systems are one of the most used technologies to cover the increase of the demand [2]. Moreover, the implementation of new renewable power plants has increased more rapidly compared with other energy technologies, and it is estimated that this will further increase by 36% to 2021 [1].

The growth in the use of renewable energy in the electricity market has many advantages both in the present and in the future. For instance, renewables reduce the carbon emissions of the power sector, and its quick implementation is key to accomplish the decarbonisation necessary for the 2SD scenario (get a probability not less than

50% that the maximum increase in temperature will be not more than 2°C by 2100) [2]. Moreover, the use of renewable power generation reduces air pollution and increases the energy independence, among others [1]. On the other hand, because of the variability of the renewable energy resource, a high proportion of renewable generation added to the electrical system will result in large supply fluctuations to the power system and a mismatch between supply and demand [3]. To avoid fluctuations, the intermittent generation from renewable energy can be integrated with energy storage in order to accumulate energy during hours with excess of generation and use it when energy is needed, providing a dispatchable or baseload generation from renewable energy technologies [4].

In power systems, energy can be stored in different forms: Mechanical, Electrochemical, Electrical, Chemical or Thermal [5]. Nowadays the most used technologies in the electrical grid, due to its technical and financial performance in large scale integration, are different kinds of mechanical energy storage (pumped hydro, compressed air energy storage, flywheel) and chemical energy storage (hy-

*Corresponding author

Email addresses: r.bravo@ed.ac.uk (R.Bravo),
d.friedrich@ed.ac.uk (D.Friedrich)

¹The author is supported by a PhD student scholarship from BE-CAS CHILE, CONICYT.

drogen, synthetic natural gas) [5], [6]. Moreover, depending on the required application (time-shifting, electric supply capacity, load following, regulation, etc.), energy storage systems can be integrated in different areas of the electrical grid: generation, transmission, distribution, or in the customer side [6]. In renewable energy power plants, energy storage systems can be applied to the system under two objectives: injection profiling (time-shifting) or injection smoothing (capacity firming) [7].

Energy storage technologies that are suitable or under developed for renewable energy projects focusing on both time-shifting and injection smoothing, are batteries, flywheels [6] and thermal energy storage [4]. One of the prominent technologies that are plausible in the near future to be included in large scale renewable energy power plants are batteries such as Lithium-ion technology [1]. Nowadays, a large scale battery infrastructure is at least one or two orders of magnitude more expensive than thermal energy storage [8]. In fact, thermal energy storage (TES) is a key technology that has been implemented in concentrating solar power plants (CSP) to store heat and deliver energy in form of heat or electricity, increasing the dispatchability of solar power plants and promoting the integration of renewable energy power plants [9].

Large scale commercial concentrating solar power plants have been operating in California since the 1980s and some of these power plants are still in operation [10]. Four different concentrating solar power technologies are commercially available and have been developed and implemented from small scale to utility scale projects around the world, i.e. solar tower, parabolic trough, linear Fresnel reflectors and dish/engine systems [11]. During recent years, solar tower technology has shown an interesting development, and the largest solar power plants in operation or under development are based on this technology. For instance, the Crescent Dunes power plant, located in Nevada, which started its operation in 2015, is one of the first large scale CSP power plants to supply almost continuous electricity by using a single tower, a 110 MW power block, and thermal energy storage equivalent to 10 hours of full power [12].

The process in these CSP plants begins in the solar field, where a large number of strategically located heliostats (two axis tracking mirrors) concentrate the sunlight in a chamber located on the top of a tower. In this chamber, known as receiver, the energy from the solar radiation is transferred to a heat transfer fluid (HTF). Then, the two-tank energy storage system allows the possibility to store the energy from the hot HTF to be used later. Hence, after leaving the chamber, the HTF is pumped to the hot tank to be transferred to the storage medium for later use or used directly as a heat injection in a Rankine cycle, through a heat exchanger. Next, the "cold" HTF is pumped directly to the tower and heated through the receiver, or it is used to reduce the temperature in the cold tank. In the Rankine cycle, superheated steam is produced in order to run a turbine and generate electricity. Regard-

ing the energy storage system, the two-tanks molten salt system has been used in most of the CSP plants [13]. Furthermore, depending on the design, molten salts can work as both the HTF and also as the storage medium.

In order to reach the desired performance, CSP technologies need high values of direct normal irradiation, for instance, to produce around 1 kWh_e per m^2 per day, the solar field of the CSP plant needs a DNI greater than $7 \text{ kWh m}^{-2}\text{day}^{-1}$ [10]. Areas with clear skies close to the Tropic of Capricorn and Cancer, between north or south latitudes of 15 and 40, present the best conditions for its operation [10]. Nowadays, large power plants that are in study, development and under construction are located in these zones, for example, the south-western United States (California, Arizona), Tunisia, Chile, among others [11], [14], [15]. Some of these projects integrate thermal energy storage, while other designs consider hybridisation. For instance, Atacama-1 or Cerro Dominador Solar Power Plant, located in Northern Chile, will supply firm electricity by combining CSP with thermal energy storage, capable to deliver energy at full working capacity for 17.5 hours. In addition, hybridisation was designed by integrating a photovoltaic (PV) power plant [16]. While energy storage systems allows full dispatchability, hybridisation offers performance benefits and synergies. It improves both technical and financial performance by integrating a cheaper technology, e.g. PV, with a more expensive, but dispatchable technology, e.g. CSP with TES [17], [18]. In the long term, due to cost reduction of batteries, the integration of battery energy storage systems with PV power plants could be key to develop dispatchable power plants with improved financial performance. However, due to the current high cost of batteries for PV compared with TES for CSP, batteries will not be evaluated in the current research [8].

As a pathway to a cost-competitive decarbonisation for electricity generation, a co-firing option can be included into a CSP plant in order to get a firm power supply, working even with no solar irradiation, hence, increasing its dispatchability. However, the current model focuses on the performance of power generation only from solar technologies. Some research demonstrate that hybrid systems integrating high cost CSP with TES and low cost PV power plants can be key to provide competitive dispatchable large scale energy generation [17], [19]. Moreover, the operational optimisation of solar tower systems integrated with thermal energy storage and hybridised with photovoltaic power plants allows to reach high capacity factors [20], [21]. Many authors agree that solar energy systems integrated with energy storage is one of the most suitable sustainable technologies to provide economical, reliable, and dispatchable power [4], and that the hybridisation of such systems allows even better performance [17], [18]. Hence, the hybridisation of firm generation from CSP plants with thermal energy storage and lower cost generation from PV power plants enables excellent features like dispatchability, decreases the intermittent generation from

renewables, match supply and demand, as well as decrease the levelised cost of electricity from solar power plants.

In pursuance of reaching high dispatchability as well as low cost of energy generation, several studies focusing on implementation of CSP with TES in different areas have been published in recent years. Some of them are focused on the optimisation of the design and its operation through different modelling approaches (linear programming, neural networks, evolutionary algorithms, non-linear modelling). For instance, [22] developed different thermodynamics configurations in order to model the behaviour of the thermal energy storage in a small-scale power plant that supplies constant heat for industry applications, minimising the thermal losses of the system. In order to optimise the design of a solar power plant by sizing its elements, [23] employs artificial neural networks and a genetic algorithm to maximise the financial performance of the project. [24] evaluated the possibility to supply electricity and heat in an off-grid scheme for a large scale copper mine, Collahuasi, one of the largest copper mines located in Chile [25]). This research was focused in the optimal selection of the best technology of an integrated solar power plant (CSP and PV) with energy storage (pumped hydro energy storage, advanced adiabatic compressed air storage, and thermal energy storage), minimising the investment of the complete system to ensure the supply of energy. Other studies demonstrate the suitability of CSP with TES, for example in Northern Chile, to work as baseload power as well as the benefits for the grid [26]. Moreover, the Atacama Desert is one of the most appropriate places to develop CSP plants due to high levels of direct normal irradiation [27], [21].

Previous studies do not exploit the synergies of large scale hybrid renewable power plant systems by simultaneously optimising financial and technical performance in both, the design and the operational optimisation stages. In order to optimise the design of a power plant regarding defined objectives, the operation of the power plant has to be optimised focusing on the same objectives. For instance, if the objectives are related with financial and reliability performance, i.e. the trade-off between the cost of the energy and the reliability of the power plant, the optimal design of a project requires a multi-objective optimisation of both the operation as well as the design in a two stage process. The first optimisation stage should find the optimal operational profile for a given design, e.g. maximising the energy delivered of a defined power plant (that means minimising the cost of the energy) and maximising its reliability. In the second optimisation stage, the design is modified with the aim of designing a power plant with low cost of energy and high reliability.

While the small number of design variables enables the use of nonlinear, multi-objective methods for the design optimisation, the operational optimisation requires the use of linear programming methods. This is due to the large number of optimisation variables, e.g. 8760 for a yearly operation profile with hourly resolution, which make the

problem intractable with optimisation methods for nonlinear problems. However, the standard linear programming methods are only capable of single objective optimisation and thus previous studies have only considered single objective, two-stage optimisation of PV and CSP with TES systems. The aim of this research is to fill this gap, by optimising at the same time the design and operation of a hybrid solar power plant composed of a CSP plant with TES and a PV power plant with respect to multiple objectives.

In this paper a two-stage optimisation in which a multi-objective operational optimisation is used to supply the operational information to a multi-objective design optimisation is presented. The results of the optimisations are Pareto fronts which show the trade-offs of different designs with respect to different technical and financial performance metrics of hybrid solar power plants. The Pareto fronts show the effects of different designs and enable the design of hybrid solar power plant that balance economic and reliability requirements.

Abbreviations

DNI: Direct normal irradiation
 GII: Global incidence irradiation
 TMY: Typical meteorological year
 CSP: Concentrating solar power
 PB: Power block
 PV: Photovoltaic
 TES: Thermal energy storage
 SM: Solar multiple
 StH: Storage hours
 CF: Capacity Factor
 LPS: Loss of power supply
 LPSC: Loss of power supply capacity
 LPSP: Loss of power supply probability
 LCOE: Levelised cost of electricity
 TLCC: Total life cycle costs
 CRF: Capital recovery factor
 SoC: State of Charge

Nomenclature

i : period (hours)
 t : period (years)
 DNI_i : Direct normal irradiation period i
 GII_i : Global incidence irradiation period i
 A_{CSP} : Solar field area
 E_{max}^{STO} : Storage capacity
 P_{max}^{PB} : Power block capacity
 P_{max}^{PV} : Photovoltaic power plant capacity
 Δt_i : delta time period i
 P_i^{gen} : Power generation period i
 E_{tot}^{gen} : Total energy generation
 P_i^{demand} : Power demand period i

E_{tot}^{demand} : Total energy demand
 CF_{CSP} : Capacity factor CSP plant
 CF_{PV} : Capacity factor PV plant
 $\eta^{DNI \rightarrow CSP}$: Efficiency CSP solar field (from irradiation in heliostats to receiver)
 $\eta^{CSP \rightarrow PB}$: Efficiency CSP plant (from receiver to power block)
 $\eta^{STO \rightarrow PB}$: Efficiency TES (from TES to power block)
 η^{TES} : Efficiency TES (self discharge)
 η^{PB} : Efficiency PB (th to el)
 $\eta^{GII \rightarrow PV}$: Efficiency PV array
 η^{INV} : Efficiency INV (DC to AC)
 LPS_i : Loss of power supply period i

2. Framework description

In the present section, a description of the power flow model of a hybrid solar power plant is explained. Then, details on the implementation of the optimisation of the operation of such power plants are given. After that, a two-stage design and operational optimisation is presented.

2.1. Power flow model

In order to optimise a hybrid solar power plant, it is necessary to study the thermodynamic performance of the process for a given location. The performance of the hybrid solar power plant for different configurations and conditions is calculated with a power flow model.

The structure used in modelling a hybrid solar power plant which integrates a concentrating solar tower plant with a two-tank thermal energy storage system and a photovoltaic power plant is shown in Figure 1. This power flow model exposes the processes involved in the operation of this type of solar power plant in terms of power flows, energy balances, energy losses, and capacities of components. In the power flow model presented, every block is one of the main subsystems of the power plant: solar field of the CSP, thermal energy storage system, power block (PB), PV power plant, inverter, and network. Every line that connect two subsystems represent heat or electricity transfer. Parameters are given by blue letters, and these are associated with solar resource (DNI, GII) and efficiencies of the pipes, power lines, or subsystems. Constraints are related with the capacities of different subsystems or components. The three heat flows (from the CSP to the PB, the CSP to the TES, and from TES to the PB) are optimisation variables which are optimised with respect to the objectives of the operational optimisation. Other variables like the amount of curtailed energy in the CSP plant when the storage system is full and when the power block is working at full capacity, as well as the thermal losses in the TES system or in the lines and the energy dispatched by the PV power plant are calculated by energy balances according to the results of the optimisation. The optimisation of the design of the power plant is represented in the

model by the optimisation of the capacities of four subsystems: solar field area of the CSP, storage system, power block, and PV power plant, and these are optimised in a second stage. Finally, the model focuses in supply energy to a given Load, which is considered as a commitment, moreover, the excess of generation has no penalty and can be delivered to the network

The parametric model developed in this study considers a typical meteorological year (TMY) with hourly resolution to represent the long time solar resource performance of the location under consideration. According to [28], designers and developers, in order to evaluate the feasibility of a solar power plant project in a particular location, frequently use the TMY, which represents the condition of the site in study through an annual data set. Moreover, the TMY is included in open data source in the countries mentioned above (Chile, United States) [29], [8]. However, while TMY is a valuable indicator that represents the conditions of the location during a long period of time, it does not show the performance of a particular year. Thus simulations based on the TMY are not able to evaluate worst case scenarios of the performance of solar power plants [28].

The parameters used to model the system are:

- DNI data of the location
- GII data of the location for a defined slope
- The efficiencies of each component
- Demand that the power plants should dispatch: P_i^{demand} (in order to calculate LPS_i)
- Operational and local limits, e.g., capacity of the network.

The power flow model is used in the optimisation of the design of the hybrid solar power plant. The optimal plant is reached by selecting the best sizes of each subsystem, i.e. solar field area, thermal energy storage, power block, and photovoltaic array. At the same time, the optimised operation of a particular design has to be performed. Therefore, a two-stage optimisation model is necessary in order to simultaneously optimise the operation and the design of the hybrid solar power plant. A schematic of this is shown in Figure 2.

2.2. Operational optimisation

The aim of the operational optimisation is to find the specific operation at each time step that enhances the performance of a hybrid solar power plant for a given design. For example, the objectives can be related with financial (cost of the electricity, investment), and/or technical (reliability) performance.

As detailed previously, and shown in Figure 1, the results of the operational optimisation are related to power flows from each element considering energy balances and the capacity of its components. The constraints are related

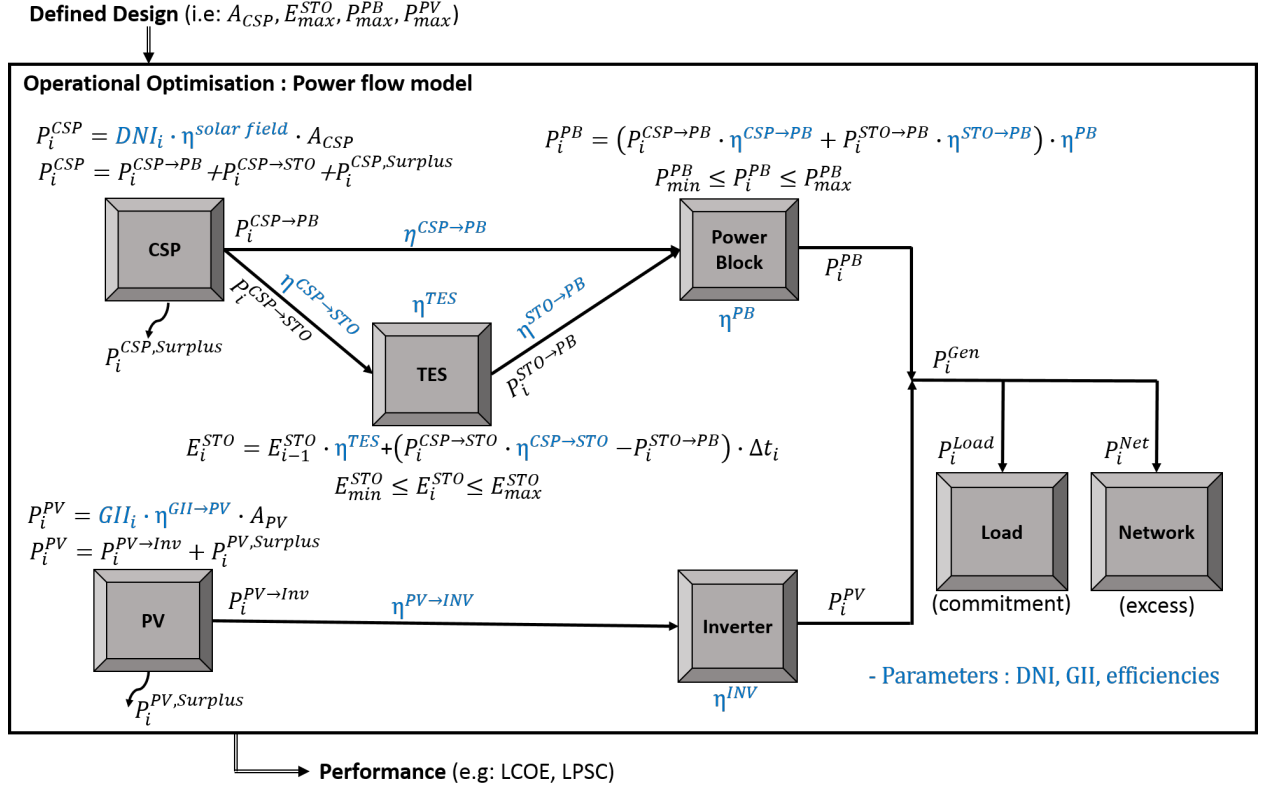


Figure 1: Power flow model hybrid system

to energy balances and maximum power flows given by the capacities of the components. For instance, the maximum power dispatched by the CSP plant has to be equal to the capacity of the power block. The variables that the model optimises are associated with the operational profile of the system, i.e. power flows between each subsystem.

The objectives of the optimisation of the operation of a given system are related to the optimisation of its technical performance, some of the properties or indicators that can be used as objectives are:

- Total energy generation: E_{tot}^{gen}
- Capacity factors of the CSP and PV plants: CF_{CSP}, CF_{PV}
- Loss of power supply capacity: $LPSC = \sum_{i=1}^I LPS_i \Delta t_i$
- Loss of power supply probability: $LPSP = \frac{LPSC}{E_{tot}^{demand}}$

In order to calculate the LPSC and LPSP, the loss of power supply of period i (LPS_i) with $i \in [1, 8760]$ is necessary. This variable is defined as 0 when generation exceed demand, and by the difference between the demand that should be dispatched in period i (P_i^{demand}) and the generation of the same period P_i^{gen} when demand exceed generation:

$$LPS_i = \begin{cases} P_i^{demand} - P_i^{gen} & , P_i^{demand} > P_i^{gen} \\ 0 & , \text{otherwise.} \end{cases}$$

Linear programming methods are used to find the power flows which optimise the given objective. This objective and further calculated properties, e.g. LPSP, are returned and can be used in the design optimisation. The operational optimisation needs to be performed by linear programming due to the large number of optimisation variables: 8760 optimisation variables for each connection in Figure 1 for an annual operational profile with hourly resolution. However, linear programming solvers can only handle a single objective so that multiple objectives can only be added as constraints or through weighting of objectives.

2.3. Design plus operational optimisation

The aim of the design optimisation, defined as a two-stage optimisation problem, is to have the best or a range of designs of hybrid solar power plants that optimise the pursued objectives. The design optimisation needs to simultaneously optimise the operation of each candidate and focus on the selection of the best designs. This is done by the operational optimisation described above, and its results are the input data to select the best range of designs. In other words, the operation of each configuration of the design optimisation is optimised by the operational optimisation.

Depending on the number of objectives, the design plus operational optimisation can be modelled as single

or multi-objective optimisation. Whilst the single objective optimisation gives the best design that optimises the objective, the multi-objective optimisation reach a range of non-dominated or Pareto optimal solutions, which represent the best design for a defined trade-off between objectives. In other words, every point in the Pareto frontier is valuable and a potential candidate, hence, the next step to finish the multi-objective optimisation is a posteriori selection of the best design regarding the desired target, which has to be done by the user of the model.

2.3.1. Objectives

The objectives of the design optimisation can be related to technical (described for the operational optimisation), financial, environmental or societal performance metrics. This research is focused on technical and financial performances; however, other indicators related to environmental or societal performance can be calculated for each design outside the design optimisation and used in the a-posteriori selection in order to pick the most appropriate design from all the potential candidates of the multi-objective optimisation.

Financial performance is fundamental to evaluate the system and to compare it with the market as well as other available technologies. Some examples of financial performance metrics that can be used to evaluate the project during its lifetime are:

- Investment
- Levelised cost of energy: LCOE (for a given annual discount rate and lifetime)

The levelised cost of energy is the present value of the cost of every unit of energy produced during all the lifetime of the power plant. Considering a constant annual energy production during the lifetime of the project, the LCOE can be simplified by [30]:

$$\text{LCOE} = \frac{\text{TLCC}}{E_{\text{tot}}^{\text{gen}}} \cdot \text{CRF}(i, n)$$

Where, TLCC is the total life cycle costs, and CRF is the capital recovery factor which depends on r (annual interest rate) and N the lifetime of the project $\text{CRF} = r/[1 - (1 + r)^{-N}]$.

Environmental performance should be an important indicator of any sustainable project. Key indicators of a project can be given by:

- Reduction of carbon emissions (compared with the emissions of the local network)
- Use of water (important in locations with restricted availability)
- Reduction of other contaminants

Societal indicators are key in projects that are focusing on social development as well as economics and environmental performance. Some societal targets are:

- Creation of local jobs during the construction and operational phases
- Visual impact
- Security level of the sustainable energy system

Because the present model is a numerical approximation of the best design, each objective has to be quantitative, hence, qualitative social or environmental goals have to be represented by numerical values.

2.3.2. Decision Variables

The decision variables of the design optimisation are:

- Solar field area: $A_{\text{CSP}} \text{ m}^2$
- Storage capacity: $E_{\text{max}}^{\text{STO}} \text{ MWh}$
- Power block capacity: $P_{\text{max}}^{\text{PB}} \text{ MW}$
- PV power plant capacity: $P_{\text{max}}^{\text{PV}} \text{ MW}$

Some of these variables are related to each other under the following indicators, which can be key to understand and define the features of optimised plants:

- SM, Solar multiple. Defined by [4] as the relation between the design capacities of the solar field and the power block.
- StH, hours of storage. Is the ratio between the total capacity of the storage system (MWh) and the power block capacity (MW).

2.3.3. Optimisation method

In order to model the design optimisation, a genetic algorithm was used. This mathematical process is shown in Figure 2, explaining a two-stage mathematical optimisation model of the design of the power plant by genetic algorithms and of the operation of the power plant by linear programming. The optimisation starts generating a random population of a defined number of individuals, this means that each individual is a particular solar power plant, i.e. a hybrid solar power plant with a defined size of the solar field area (m^2), the storage size (MWh_{th}), the power block (MW_e), and/or the photovoltaic power plant capacity (MW_e). After that, the algorithm evaluates each individual under the operational optimisation model previously described and measures the performance of each individual regarding the objectives of the design optimisation problem. Then, the genetic algorithm defines the best offspring by crossing and mutating the population in which power plants with better performance have higher chance to evolve. Finally, the end condition is associated with a defined number of generations which is given to the model as an instruction.

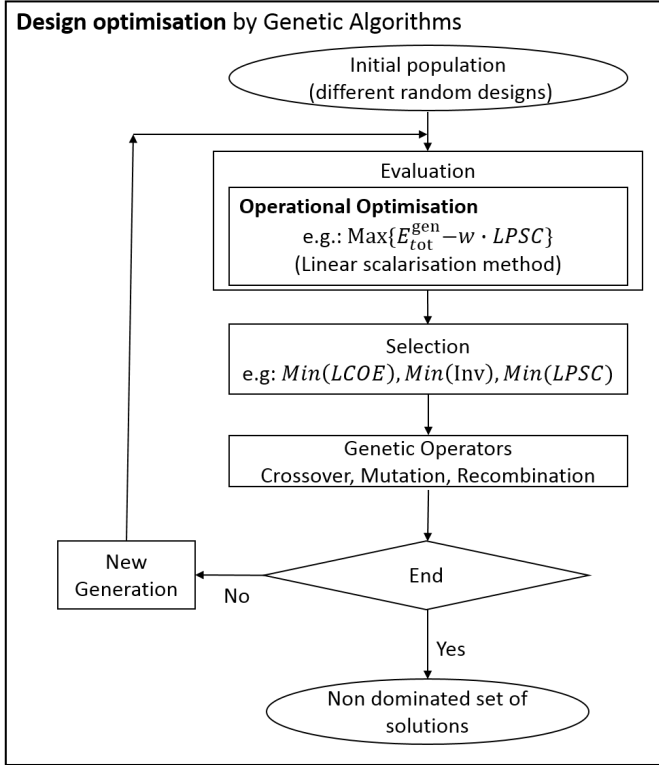


Figure 2: Multi-objective optimisation framework

2.4. Computer information

All simulations and optimisations were performed with the following hard- and software:

- PC: Intel Core i7-6700 3.4 GHz and 16 GB RAM
- Operating system: 64-bit Windows 7
- Programming language: Python 3.5.3
- Optimisation packages: Pyomo with CPLEX and Gurobi, DEAP

3. Results

3.1. Case Study

In order to set a case study, the Atacama Desert will be considered. This arid region which covers around 300,000 km² is located in Northern Chile, and is one of the sunniest places on Earth [31], where in a typical year, the annual Direct Normal Irradiation (DNI) is near or more than 3,500 kWh m⁻² [29], [15]. In this zone are located 23 of the 30 bigger copper mines of the Chilean copper industry [25], which accounts for around 73% of the copper production in Chile, whereas this Chilean industry contributes more than 30% of the total copper production of the world [32]. This copper industry is a continuous and energy intensive process, in fact, during 2015, Chilean copper mines used around 23,600 GWh of electricity and additionally around 2,700 GWh was burned as a fossil fuel

for low temperature heating operations mainly in copper refining and hydrometallurgical processes [33]. Because the mining industry leads the electricity consumption in Northern Chile, the demand is quite flat, with no significant variations between day and night, hence, the Northern Chile electricity market needs to supply a steady energy demand 24 hours and 7 days per week. Regarding the Chilean Center for Economic Load Dispatch (CDEC) of the Northern Interconnected System (SING), 75.4% of the electricity generated during 2015 was generated in coal-powered power plants, 21% from other fossil-fuelled power plants (Natural gas, Diesel, Fuel Oil), and just 3.6% from renewable resources (solar, wind, hydro) [34]. According to these numbers, the Chilean Ministry of Energy reported that the carbon intensity of the SING in 2015 was 0.764 tCO_{2eq} MWh⁻¹ [35]. On the other hand, one of the biggest challenges of the Chilean mining industry is to get economical, reliable, and sustainable energy resources, as well as the efficient use of them [25]. To apply and prove the model, the Atacama-1 or Cerro Dominador Solar Power Plant, a hybrid solar power plant under construction in the Atacama Desert in Chile has been studied. Regarding the published information by the constructor company [16] and by the Chilean Ministry of Environment [36], some features of the project are:

- **Location:** Antofagasta Region, Chile ≈ S 22° W 69°
- **CSP Plant**
 - Heliostats: 10,600 ≈ 148.4 ha
 - StH: 17.5 h
 - Power Block Capacity: 110 MW
- **PV Plant:** Capacity: 100 MW
- **GHG emissions avoided:** 870,000 tCO_{2eq} year⁻¹
- **Total Investment:** between 1,300 and 1,500 MUSD

3.1.1. Solar Irradiation Data

The DNI and the GII (for a panel slope ≈ latitude) data in the location of the project was obtained from the Chilean Ministry of Energy and University of Chile solar resource data centre [29]. This open source information includes weather and irradiation data of the Chilean territory.

Figure 3 shows the moving average of 1 and 2 days in the location. In both cases, the 5th percentile is around 330 Wh m⁻², this means that 95% of the time the DNI is at least 330 Wh m⁻² day⁻¹, in other words, the daily DNI has no great variation during the year. The present study considers the typical meteorological year, hence, the results represent the long time performance of the project. Nevertheless, the irradiation variability in the Atacama Desert is influenced by El Niño-Southern Oscillation (ENSO). While La Niña has a high correlation with high precipitations

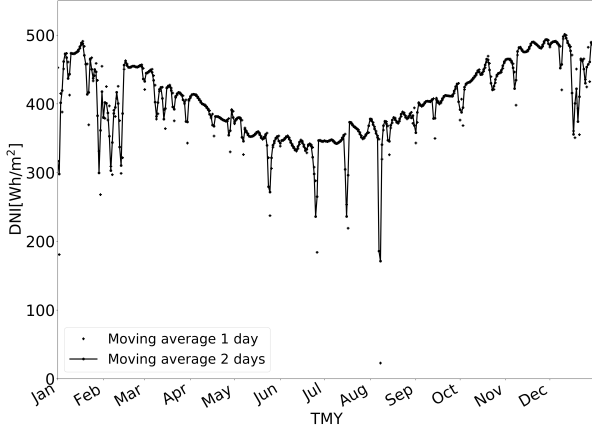


Figure 3: Moving average of the solar irradiation for the typical meteorological year

during summer (Dec-Jan-Feb-March) of the Southern Hemisphere in the Atacama Desert between a six years interval, high rainfalls during winter are associated with El Niño [37]. These phenomena will result in years with solar irradiation significantly different from TMY. The effect this has on the hybrid solar power plant will be evaluated in a future publication.

3.1.2. Solar Power Plant Features

Technical and financial information of solar power plants in operation and under construction is necessary to build the model. The System Advisor Model (SAM) [8] was used to get financial (unitary costs) and technical (efficiencies) data to build the model. In the model, the investment cost is calculated by scaling the unitary cost of the components of the CSP and the PV power plants, e.g. USD m^{-2} for the solar field, USD MWh^{-1} for the thermal energy storage system, USD MW^{-1} for the power block, among others. Around 70% of the total annual daytime hours the DNI is greater than $800 Wh m^{-2}$, moreover, the operational optimisation is focused on maximising the use of the power plant, hence the power block will work near full capacity most of the time. For these reasons, and in order to simplify the model, the efficiencies used for each subsystem are constant for every hour and every design, these are shown in Table 1. These efficiencies are used to estimate the sizes of the components and the operational performance of the system. In order to validate the model, results of the model were compared with both, the System Advisor Model and information published by the IEA in the report: Projected Cost of Generating Electricity 2015 edition [38].

Table 1: Efficiencies used in the model

CSP Plant	PV Plant
$\eta^{solar\ field}=0.48735$	$\eta^{panel}=0.1806$
$\eta^{pipelines}=0.99$	$\eta^{PV \rightarrow INV}=0.85048$
$\eta^{TES}=0.99$	$\eta^{INV \rightarrow NETW}=0.9726$
$\eta^{PB}=0.3708$	

3.2. Operational optimisation - CSP and PV plant

The design of the CSP plant of Atacama-1 has a solar multiple of 2.59, and a storage capacity equivalent to 17.5 hours of full capacity. The operational optimisation model was first applied to the CSP plant of Atacama-1. The parameters used were the typical meteorological year of the location reported by [29], a discounted rate equal to 7% and 25 years of lifetime (in order to compare the results with the IEA report [38]). The model was run twice with two different objectives: $Max\{E_{tot}^{gen}\}$ and $Min\{LPSC\}$ (for a fixed constant supply of 110 MW, which correspond to the maximum capacity of the power block), these results are shown in column CSP in Table 2.

Because E_i^{demand} is equal to the capacity of the power plant, both $Max\{E_{tot}^{gen}\}$ and $Min\{LPSC\}$ obtain the same results. Nevertheless, if E_i^{demand} were variable and not equal to the capacity of the power plant, or if the local electrical market had variable electricity cost during the day, the optimisations with different objectives would produce different results. These different cases, that depend on the market in which the system will operate, can be modelled by adjusting the input parameters of the programme.

In the case of the PV plant of Atacama-1, the one year operational optimisation results, similarly to the CSP plant, are the same for both objectives: $Max\{E_{tot}^{gen}\}$ and $Min\{LPSC\}$ (for a constant supply of 100 MW which is the maximum capacity of the plant), these results are shown in the column PV in Table 2.

3.3. Multi-objective Operational Optimisation - Hybrid plant

The objectives defined in the model depend on the target pursued by the owner of the power plant. For instance, the user of the model can be focused just on a financial perspective by selling the maximum quantity of energy, thus, reaching the lowest LCOE. On the other hand, the case that the owner of the power plant is a large consumer, its objectives might be focused on both financial and reliability performance. In addition, these will be different for grid connected or off-grid power plants. Finally, the electricity market operator will be focused on both, a low price of the electricity, as well as a firm electricity supply, which can be evaluated through the LPSC. The operational optimisation developed in this model will focus on a combination of these two objectives, the maximisation of

Table 2: Operational optimisation Atacama-1

KPI	unit	CSP	PV	Hybrid		
				$Max\{E_{tot}^{gen}\}$	$Min\{LPSC\}$	Autom.Scalarisation
E_{tot}^{gen}	GWh year ⁻¹	864.3	261.4	1,125.7	953.8	1,109
LPSC	GWh year ⁻¹	99.3	615.9	97.5	9.8	9.9
LPSP	%	10.30	72.30	10.12	1.016	1.02
CF _{CSP}	%	89.69	-	89.69	71.85	87.98
CF _{PV}	%	-	27.12	27.12	27.12	27.12
Investment	MUSD	1,192	262	1,455	1,455	1,455
LCOE	USD MWh ⁻¹	132.06	92.40	122.85	144.04	124.60

the energy supplied (low cost of electricity) and the minimisation of the loss of power supply.

In this context, the previous results show that CSP with TES plants have higher LCOE but lower LPSC than PV plants (because energy can be stored in the CSP plant and used during night hours), hence, the combination of these two solar power plants should mean both better financial and technical performances. Consequently, a decrease in both LCOE and LPSC is expected by the hybridisation. In this case the maximum capacities of both power plants are different, $P_{max}^{PB} = 110$ MW and $P_{max}^{PV} = 100$ MW. Besides, the E_i^{demand} was defined fixed and constant at every hour and equal to the maximum capacity of the CSP power plant (110 MW), because unlike the PV plant, the CSP plant with thermal energy storage system can deliver energy during the night. Therefore, both methods: $Max\{E_{tot}^{gen}\}$ and $Min\{LPSC\}$ get different results, which are summarised in Table 2.

First, the $Max\{E_{tot}^{gen}\}$ method achieves the highest total energy generated (1,125.7 GWh year⁻¹), consequently, the minimum LCOE, but the LPSP is high (10.12%). Second, the $Min\{LPSC\}$ results in a very low value in both LPSP (1.016%) and E_{tot}^{gen} (953.8 GWh year⁻¹), consequently, a higher LCOE. The hybridisation of the power plant should be able to give a better performance. However, the right operational strategy of the hybrid solar power plant is essential in order to simultaneously maximise the energy delivered to the network (which influences the LCOE) and minimise the LPSC (which influences the reliability of its operation). For that reason, a multi-objective optimisation algorithm, showing the trade-off between financial and technical performance is needed, in order to reach better results.

Two techniques have been applied to solve multi-objective optimisation problems in the linear programming operational optimisation [39]: the weighted-sum or scalarisation method, and the ε -constraint method. Whilst in the scalarisation method, the multi-objective optimisation problem is transformed to a single objective optimisation problem by combining and weighting both objectives [40], in the ε -constraint method, one objective is considered as a constraint in the formulation of the optimisation problem [41]. One important challenge of these methods is to define

the correct value of the scaling or constraint parameters in order to get suitable solutions. Moreover, the result of a multi-objective optimisation problem is a Pareto frontier (or surface) which represents a set of points that are solutions to the problem, ergo, every point is an optimal candidate with exclusive features regarding the objectives. These methods, which are modelled and applied to the hybrid power plant, are described below.

3.3.1. Scalarisation method

The following function describes the new single objective optimisation problem:

$$\text{maximize} \quad \sum_{i=1}^I \{P_i^{gen} \Delta t_i - w LPSC_i \Delta t_i\}$$

Where the positive parameter w is the scaling factor applied to the second objective. Regarding the results shown in Table 2, the scaling factor that balances the second objective ($LPSC_i$) with respect to the first one (P_i^{gen}) can be approximated by

$$\frac{E_{max} - E_{min}}{LPSC_{max} - LPSC_{min}} = \frac{1,125.5 - 953.8}{97.5 - 9.8} = 1.96$$

Hence, in order to build the Pareto frontier, and compare the solutions of this method with the previous results of the single objective optimisations, w was evaluated in the range $w \in [0, 100]$, which is large enough to cover the range between the two single objective optimisations. The Pareto frontier generated from this method is presented in Figure 4.

3.3.2. Epsilon constraint method

In this method the optimisation problem is formulated as:

$$\begin{aligned} &\text{maximize} \quad E_{tot}^{gen} \\ &\text{subject to} \quad LPSC \leq \varepsilon \end{aligned}$$

Where ε varies between the values of the LPSC given by both previous single objective optimisations shown in Table 2: $\varepsilon \in [9.8, 97.5]$ GWh year⁻¹. The Pareto optimal values generated from this method are also shown in Figure 4.

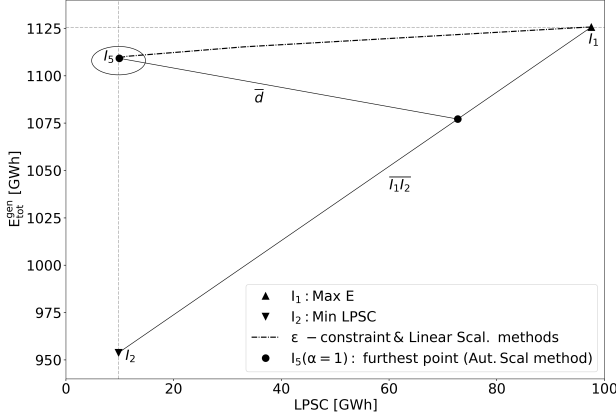


Figure 4: E_{tot}^{gen} vs LPSC, summary all methods

From Figure 4 it is possible to appreciate the behaviour of each of the 4 different methods studied: First, the $Max\{E_{tot}^{gen}\}$ method maximises the energy delivered, getting the lowest LCOE (122.85 USD MWh⁻¹), nevertheless, it presents the highest LPSP 10.12% which is not an attractive value for the reliability of the system. Second, the $Min\{LPSC\}$ method is outside of the Pareto frontier, and it presents a very low value of the total energy delivered to the network, so, the LCOE associated to this method is high and not attractive for the financial optimisation of the system. Finally, both the scalarisation and the ϵ -constraint methods show similar Pareto optimal solutions.

Because the purpose of the model is focused on a strategic point of view in which the generation company is looking for a maximisation of its profit (a minimum LCOE), and the market operator is focusing on a reliable energy system, the objective of the operational optimisation will focus on a combination of both objectives, thus, the target of the optimisation should reach the zone highlighted with an ellipse in Figure 4. Both the $Max\{E_{tot}^{gen}\}$ and the $Min\{LPSC\}$ methods do not reach this zone, on the other hand, the scalarisation and the ϵ -constraint method, with a good definition of values of w and ϵ , respectively, can reach this area. The main difference between the scalarisation and the ϵ -constraint methods is that each iteration of the scalarisation method takes a few seconds to calculate, compared with each iteration of the ϵ -constraint method which takes almost 10 minutes to be processed. Hence, to continue with the optimisation, the scalarisation method is analysed in detail and automated, to ensure that the optimal value of w is chosen.

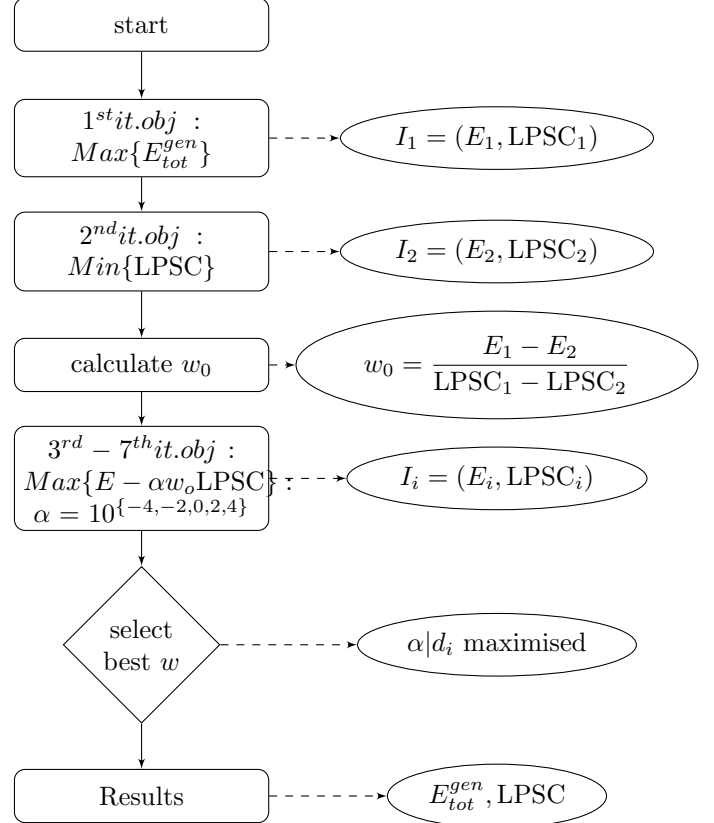
3.3.3. Automated scalarisation method

In order to have an automated decision system ensuring that the solution of the operational optimisation is in the desired zone, an automated scalarisation method was developed and applied. This autonomous algorithm requires 7 iterations. The first iteration is a single ob-

jective optimisation of $Max\{E_{tot}^{gen}\}$ and it gives the point $I_1 = (E_{max}, LPSC_{max})$ in Figure 4. Then, the second iteration is a single objective optimisation of $Min\{LPSC\}$ which produces the point $I_2 = (E_{min}, LPSC_{min})$ (Figure 4). The purpose of these first two iterations is to get both an estimation of w and the line $\overline{I_1 I_2}$. Then, the initial value of w is calculated by

$$w_0 = \frac{E_{max} - E_{min}}{LPSC_{max} - LPSC_{min}}$$

in order to give the same relative weight to both objectives. After that, 5 iterations are carried out to get an improved w ($w = \alpha w_0$) which is used as input to the a-posteriori automated selection. This last step, the automated a-posteriori selection can be modelled by different methods depending on the purpose of the user. In this case, it is done by selecting the α value for which the result ($I_i = (E_i, LPSC_i)$) of the i^{th} iteration is furthest from the line $\overline{I_1 I_2}$. This is calculated by finding the maximum distance d_i which is the perpendicular line that connects I_i with $\overline{I_1 I_2}$. The following algorithm describes this procedure:



This automated scalarisation method was applied to find the best operational profile for Atacama-1. Figure 4 summarises this method, in which the best result, or the maximum value of segment d is found for $\alpha = 1$. As a clarification, segments d and $\overline{I_1 I_2}$ are perpendicular, nevertheless, because the scale of both axes are different in the Figure 4, these do not seem to be perpendicular in the diagram.

The results of the automated scalarisation are shown in Table 2. These results, compared with the method in

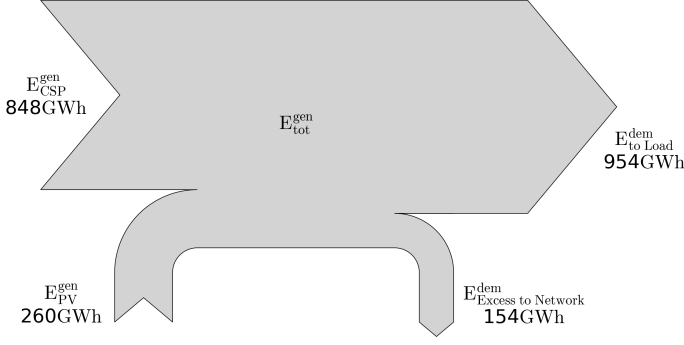


Figure 5: Annual energy flow diagram

which the objective is the $Max\{E_{tot}^{gen}\}$ means an increase in 1.4% in the LCOE, nevertheless, the LPSP is just 10% of the original (1.02% instead of 10.12%). As expected, comparing the CSP plant with the hybrid plant, the LCOE decreases from 139.06 to 124.6 USD MWh⁻¹ and the LPSP decreased from 10.30% to 1.02%.

Another useful output of the operational optimisation are the hourly power flows between each component, and the losses in each subsystem. With these it is possible to get the state of charge (SoC) of the thermal energy storage system, which is shown in Figure 6. The storage system of Atacama-1 has a StH of 17.5 h, this means that when the storage is fully charged (100%) the power plant can work at full capacity for 17.5 h with no solar irradiation. However, regarding Figure 6, the maximum state of charge of the TES system is 83%, with a mean of 36.3%. This suggests that it is possible that the TES system of Atacama-1 is oversized and its capacity could be reduced in order to reduce investment costs in the design step, which opens the possibility to improve the design of Atacama-1. Regarding the features of the thermal energy storage system, there is a lower limit of temperature that the molten salts must not reach in order to avoid its solidification. Hence, as shown in Figure 6, during cold months, where the minimum state of charge is 0 every day, special attention has to be put on the perfect operational control needed to avoid this problem.

3.4. Multi-objective design optimisation - Upgrading Atacama-1

The optimisation model was applied and run for the same location of Atacama-1. The purpose of this step is to get the best design of a hybrid solar power plant in the same location of Atacama-1 and with similar features. Table 3 summarised the components considered in the design optimisation. First, the parameters are related with the solar resource of the location, the efficiencies and unitary cost of the components given by data from power plants under construction and in operation, as well as other financial parameters like the lifetime, the discount rate, among others. Second, the constraints are associated with the application of energy balances and energy or power capacities

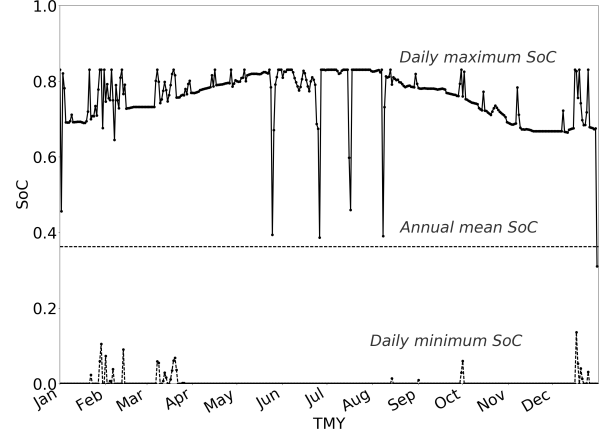


Figure 6: State of charge of the TES system

which are applied to the operational optimisation. Third the objectives can be related with the goals that the user is focusing on. Finally, the variables are related with the capacities of each component, these are the solar field area and the capacities of the thermal energy storage system, the power block and the photovoltaic power plant.

Table 3: Design Optimisation: list of parameters and constraints and all potential objectives and variables

Param.	Constr.	Obj.	Var.
DNI	Energy balances Power capacities	LCOE	A_{CSP}
GII		Investment	E_{max}^{STO}
Efficiencies		LPSC	P_{max}^{PB}
Unitary costs			P_{max}^{PV}
Financial param.			

The following results describe different methods applied to the same design optimisation problem. These depend on the number of objectives, and the number of variables. First, the number of variables considered in the optimisation can be from one variable up to four variables, related with the capacities of each subsystem. The case in which one variable is considered can be thought as an upgrade to the existing power plant in order to improve its performance. On the other hand, four variables can be considered in order to develop a brand new power plant defined by the given parameters. Second, the number and kind of objectives considered by the user. For instance, a generator company might want to increase the revenues of the power plant by reaching the lowest LCOE. Other users could be the market operator or a large consumer, which could be interested not just in the financial performance but in the reliability as well. The most complex situation is a multi-objective optimisation, in which financial, technical, environmental and/or social objectives are

pursued.

3.4.1. Single variable, single objective

As a first approximation, a single variable single objective optimisation was developed and applied to Atacama-1. In this model just one design variable is considered as a variable and the other three are considered parameters (fixed). This problem was developed as a deterministic global optimisation problem, and an improved design was reached. Table 4 shows the results reached by the design optimisation of the power plant focusing on the minimization of the LCOE, while the operation of each iteration (which correspond to a different power plant design) was optimised by the automated scalarisation method described previously, that simultaneously maximises the energy delivered and minimises the LPSC.

Variable: Solar field area. Keeping TES, PB, and PV capacities fixed, the deterministic global optimisation was run getting an improved design of the plant when the solar field area is 161.4 ha, this means 930 more heliostats than the original design (11,530 instead of 10,600), hence, a larger SM. As a results, despite the investment increase, more energy can be delivered, and more energy is available during night, thus, both LCOE and LPSC decrease

Variable: Thermal energy storage capacity. Keeping the solar field area, the PB and the PV capacities fixed, the best design of the plant is given by a decrease of the TES capacity from 5243 MWh (StH= 17.5 h) to 3503 MWh (StH= 11.7 h), achieving an LCOE= 118.78 USD MWh⁻¹. This result agrees with the previous analysis of the state of charge of the TES system. The reduction in TES capacity directly reduces the investment costs and thus has a positive impact on the LCOE. Moreover, the lower TES capacity produces two effects: (i) a decrease in the energy losses in the storage system (because less energy is stored), as a result more energy can be delivered (which has a positive effect on the LCOE), (ii) because less energy is available during night hours, less energy is delivered during this time (which has a negative effect on the LPSC), therefore, LPSC increases. The combination of all these interactions results in a small increase on the energy delivered during the day, a decrease in the energy available during night, and a considerable decrease on the investment, as a result, LCOE decreases and LPSC increases.

Variable: Power block capacity. By keeping the solar field area, TES and PV capacities fixed, the best design of the plant is reached by a decrease in the power block from 110 to 108 MW. This small change in the power block should mean a small decrease in the investment and thus a decrease in the LCOE, but an increase in the LPSC because the demand is fixed, i.e. $E_i^{\text{demand}} = 110$ MW.

In summary, all the iterations of the optimisation for the three cases are shown in the sensitivity analysis diagram in Figure 7, which shows the convexity of the model for single variables and single objectives. Moreover, this diagram illustrates the best options to improve the design

of the project with the objective of decreasing the LCOE.

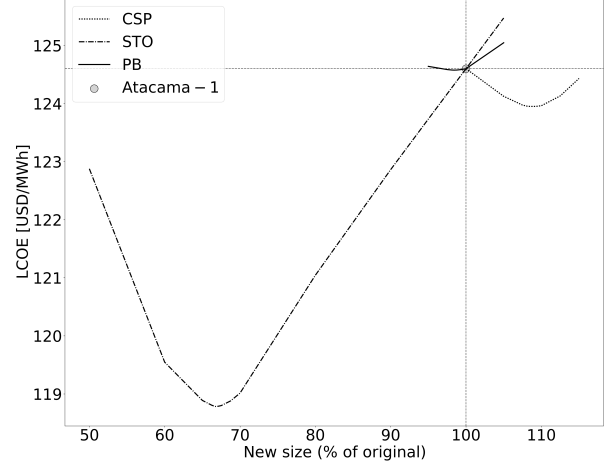


Figure 7: Results showing the sensitivity analysis of the design optimisation with 1 variable and 1 objective.

3.4.2. Multi-variable, multi-objective optimisation

The multi-variable (A_{CSP} , $E_{\text{max}}^{\text{STO}}$, and $P_{\text{max}}^{\text{PV}}$) and multi-objective (LCOE, Investment, LPSC) design optimisation is performed with the previously described genetic algorithm. This heuristic optimisation method starts with a random population (here 200 individuals), and applies the NSGA-II algorithm through a number of generations (here 80). Every individual is composed of 3 variables, corresponding to a defined design. In the algorithm, the investment related to each individual is calculated, then its optimal operational performance is achieved by applying the automated scalarisation method described previously. This simultaneously optimises the LCOE and LPSC. The selection of the best individuals is executed by the algorithm under two or three objectives: Min LCOE, Min Investment and/or Min LPSC.

The optimisation produces a range of different points that represents different options of the design of the hybrid solar power plant, and the respective performance during its lifetime (based on the TMY). Each design on this Pareto frontier represents a potential solution and the final choice will depend on the aims of the developer. In every case, in order to calculate the LPSC in the operational optimisation step, and to get results comparable with Atacama-1, the power that the generation should supply was considered fixed, i.e. $E_i^{\text{demand}} = 110$ MW. For this reason, because the CSP plant can deliver energy during the night, the power block capacity was fixed and equal to the demand, $P_{\text{max}}^{\text{PB}} = 110$ MW.

Three variables, two objectives:

The design optimisation is extended to three variables (A_{CSP} , $E_{\text{max}}^{\text{STO}}$, $P_{\text{max}}^{\text{PV}}$) and two objectives (LCOE and In-

Table 4: Design Optimisation - single variable, single objective

Indicator	unit	Atac-1	CSP	Storage	PB
New value		-	161.4 ha	3503 MWh	108.3 MW
SM	-	2.59	2.82	2.59	2.63
StH	h	17.5	17.5	11.68	17.8
E_{tot}^{gen}	GWh year ⁻¹	1,109	1,157	1,110	1,105
LPSC	GWh year ⁻¹	9.9	6.3	69.1	16.1
LPSP	%	1.02	0.65	7.17	1.67
CF _{CSP}	%	87.98	93.0	88.1	88.9
CF _{PV}	%	27.1	27.1	27.1	27.1
Investment	MUSD	1,455	1,513	1,381	1,450
LCOE (objective)	USD MWh ⁻¹	124.6	123.95	118.78	124.57

vestment cost). Figure 8a shows the results of the optimisation, the Pareto Frontier as well as the performance of Atacama-1 in order to make a quick comparison between the results. For instance, Figure 8a highlights two points (A and B) belonging to the non-dominated solutions. These solutions are detailed in Table 5, including the performance of Atacama-1 to make a quick comparison. These points are related with the best performance that can be reach with similar Investment or similar LCOE presented by Atacama-1. The first point, A, shows a design with a decrease of the LCOE and Investment, nevertheless, its LPSP is 22%. The second point, B, displays that a similar LCOE than Atacama-1 can be reached with just 65% of the original investment, but the LPSP is 37%, a very high value compared with Atacama-1.

Figure 8b shows the parameters and objectives of every point on the Pareto frontier with LPSP < 30%. On the horizontal axis are shown the 4 components of the design (P_{max}^{PB} , A_{CSP} , E_{max}^{STO} , P_{max}^{PV}), the two objectives of the design optimisation (LCOE, Investment cost), and the LPSP which is calculated from the operational profiles. The vertical axis is the normalised value of the variables, where minimum and maximum values are indicated in the figure. This figure explains that the model can reach simultaneously better LCOE and Investment cost for a design similar to Atacama-1, nevertheless, because the technical performance (represented by the LPSC) is not included in the design optimisation stage, the values of the LPSP are very high. As a consequence of these results, in order to reach better financial (LCOE, Investment) and technical (LPSC, LPSP) performance from the design optimisation, the LPSC is incorporated as a third objective.

Three variables, three objectives:

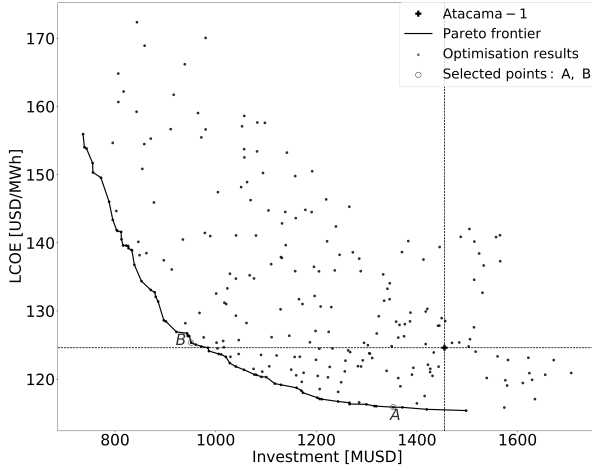
In this step, the complexity of the model is increased through a third objective, that is related with the technical performance of the hybrid power plant. Here the ability to dispatch energy when it is needed (LPSC) is added. Figure 9a shows some of the points that belong to the Pareto surface as well as the performance of Atacama-1. Only points with a performance similar to or better than Atacama-1 as defined by the following ranges are shown:

Table 5: Design Optimisation - Three variables, Two objectives

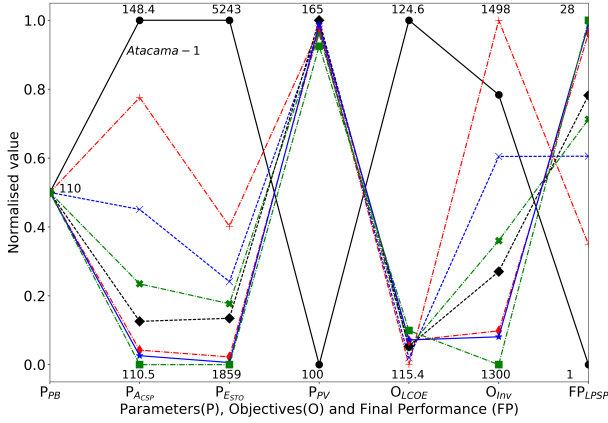
item	unit	Atac-1	A	B
A_{CSP}	ha	148.4	115.3	92.2
E_{max}^{STO}	MWh	5243	2314	1230
P_{max}^{PV}	MW	100	164	69
SM	—	2.59	2.01	1.61
StH	h	17.5	7.72	4.1
E_{tot}^{gen}	GWh year ⁻¹	1,109	1,119	742
LPSC	GWh year ⁻¹	9.9	215	363
LPSP	%	1.02	22	37
CF _{CSP}	%	87.98	71.4	58.28
CF _{PV}	%	27.1	27.1	27.1
Investment	MUSD	1,455	1,353	951
LCOE	USD MWh ⁻¹	124.6	115.9	125.3

- LPSP \leq 3%
- LCOE \leq 130 USD MWh⁻¹
- INV \leq 1,700 MUSD

In Figure 9a, the three dimensional performance (LCOE, Investment, LPSC) of the multi-objective optimisation is represented in a two dimensional diagram (LCOE, Investment), in which the third objective (LPSP) is illustrated through different ranges and symbols. Near to the centre is Atacama-1, which divides the plane into four quadrants. The crosses and the stars have a LPSP lower than Atacama-1, thus, any of them located in Quadrant I have both better financial and technical performance than Atacama-1. Second, any point in Quadrant I has better financial performance than Atacama-1, but its LPSP varies between 0.65% to 3%. Third, in order to reach lower values of LPSP (shown by crosses and stars in the diagram), similar or higher investments are needed, nevertheless, lower values of LCOE can be reached simultaneously. Fourth, whilst lower values of LCOE (Quadrants I and II) are possible with similar investments than Atacama-1, their LPSP can be even near 0.285%. For instance, five of these interesting points are summarised in Table 6 and shown in Figure 9a bounded in a circle and defined by the letters A, B, C, D



(a) Pareto optimal solutions



(b) Parameters, objectives and final performance

Figure 8: Design Optimisation: 3 variables, 2 objectives

and E. Designs A and B reach lower LCOE, nevertheless, high investments are necessary to get higher reliability, this is explained by the performance of designs A and B. Design C represents a power plants with similar investment but a lower LCOE than Atacama-1. Designs D and E are examples of very reliable power plants, which can be developed with low LCOE, nevertheless, high investment is necessary.

The 12 stars located in Quadrant I in Figure 9a, which have better financial (LCOE, Investment) and technical (LPSC) performance than Atacama-1, are detailed in Figure 9b. This last diagram shows the design parameters, the results of the three objectives and some key design indicators (SM, StH, and CF_{CSP}) as well as its comparison with Atacama-1. Moreover, for these 12 individuals a correlation matrix between each objective and key indicators of the design of the power plant (SM and StH and CF_{CSP}) was calculated and shown below:

$$corr(X, Y) =$$

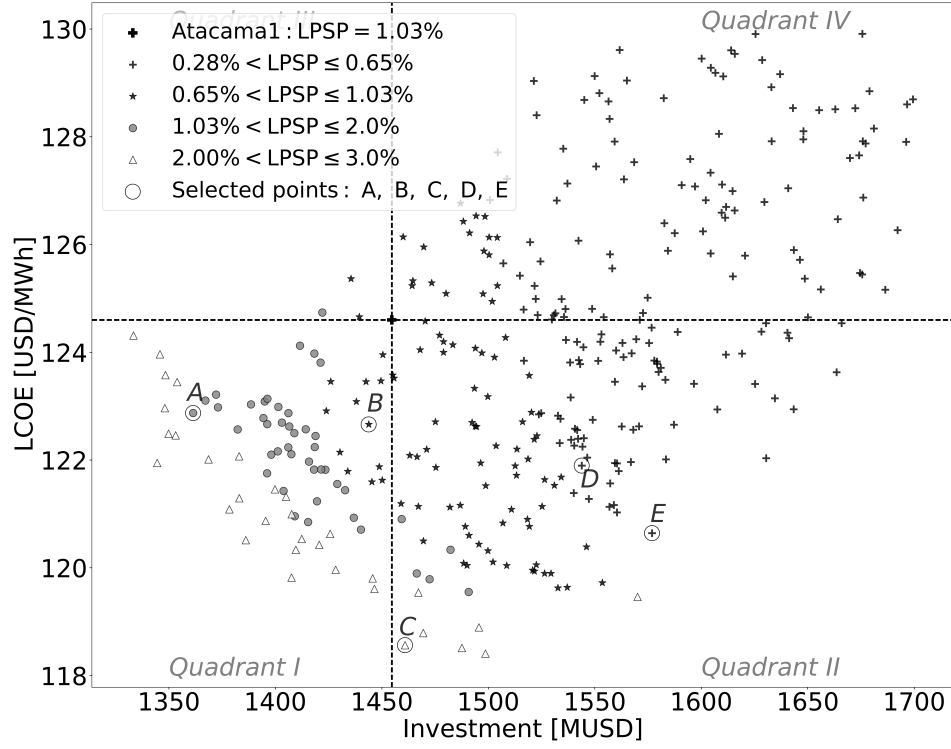
	LPSP	SM	StH
LCOE	-0.635	0.468	0.791
INV	-0.629	-0.29	0.42
LPSP	1	-0.236	-0.76
SM	-0.236	1	-0.073
StH	-0.76	-0.073	1

These results simplify the understanding of the design of the power plant, moreover, some of them are key to develop future approximations. For instance, because SM and StH are related with the installed capacities of the solar field and the storage system, both have a positive correlation with the LCOE. In relation with the LPSP, as expected, this has a negative correlation with the LCOE and Investment, in other words, in order to increase the technical performance of the power plant (decrease the LPSP or increase the reliability of the system), a decrease in the financial performance is expected (a higher value of the LCOE and/or the initial Investment). This also can be explained by the negative correlation between LPSP and both SM and StH, suggesting that lower LPSP are reached in oversized power plants. For that reason, the trade-off between technical and financial performance is important. Another interesting point is the correlation between SM and StH, which suggest that there is a positive correlation between the solar field capacity and the storage capacity observed in optimised designs.

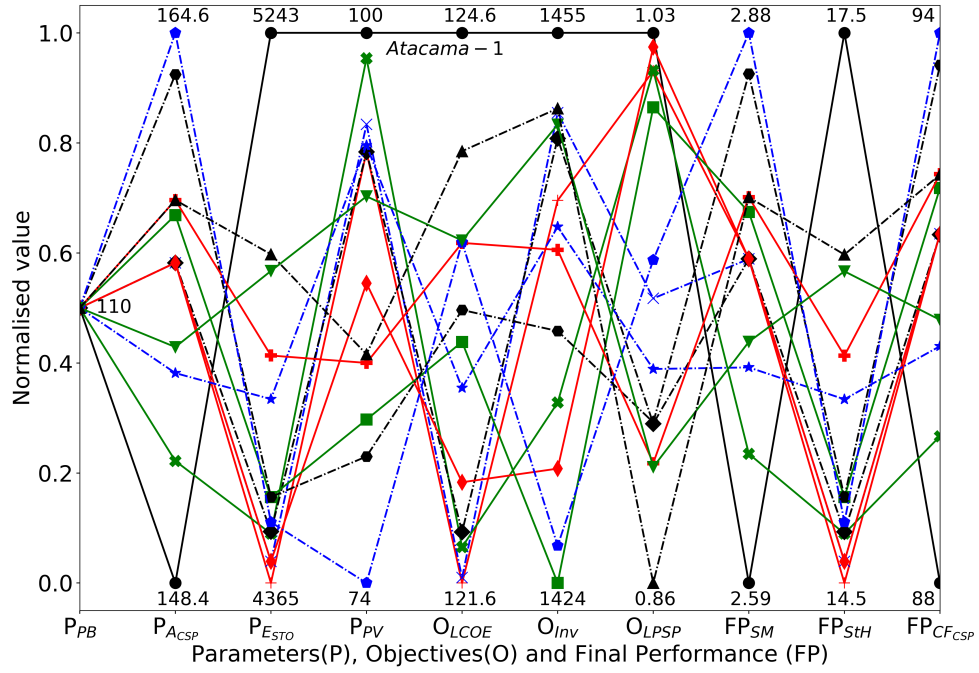
Finally, in order to have a complete picture for the a-posteriori decision, the particular design of every individual, i.e. all the capacities of the components, can be combined with key indicators of their optimised operational performance during its lifetime. In summary, Figure 9a and detailed results of the model can be used together to make a very accurate a-posteriori decision in order to select the best design with optimised performances. Because Figure 9a is a representation of the non-dominated solutions, the best decision should be made by the user.

4. Conclusion

In order to make renewable energy systems economical and reliable, the design and operation of hybrid renewable energy systems have to consider the financial and technical performance of the system and the synergies of different technologies. To achieve this, the design optimisation needs an internal routine which optimises the operational profile with respect to multiple and often conflicting design objectives. However, the operational optimisation is usually performed with single objective linear programming methods. This contribution presents a two-stage optimisation for the design of hybrid solar power plants which uses an automated scalarisation method for multi-objective linear optimisation of the operational profile.



(a) Pareto optimal solutions



(b) Parameters, objectives and final performance

Figure 9: Design Optimisation: 3 variables and 3 objectives

Table 6: Design Optimisation - multi-variable, multi-objective

item	unit	Atac-1	A	B	C	D	E
A_{CSP}	ha	148.4	151.5	154.6	146.6	157.5	164.7
E_{max}^{STO}	MWh	5243	4276	4658	3956	5040	4717
P_{max}^{PV}	MW	100	75	95	125	121	126
SM	—	2.59	2.64	2.7	2.56	2.75	2.88
StH	h	17.5	14.27	15.55	13.2	16.81	15.74
E_{tot}^{gen}	GWh year ⁻¹	1,109	1,057	1,120	1,173	1,201	1,239
LPSC	GWh year ⁻¹	9.9	19	8.9	27.5	6	5.8
LPSP	%	1.02	2.0	0.9	2.86	0.6	0.6
CF _{CSP}	%	87.98	89.44	90.51	87.58	91.64	94.06
CF _{PV}	%	27.1	27.1	27.1	27.1	27.1	27.1
Investment	MUSD	1,455	1,361	1443	1,461	1,544	1,577
LCOE	USD MWh ⁻¹	124.6	122.87	122.66	118.57	121.89	120.6

The two-stage optimisation framework developed in this research simultaneously optimises the design and operation of a hybrid solar power plant with respect to multiple objectives. The results of the design optimisation stage produce the best configuration (sizes, capacities) of a hybrid solar power plant while the operational optimisation simultaneously produces the optimal operation of the power plant. The latter can be used to analyse the hourly power flows between each component as well as the estimated losses in each subsystem. Two methods for the operational optimisation were evaluated and it was found that the linear scalarisation method achieves the same results but is much faster than the ϵ -constraint method. Then, the linear scalarisation method was automated by valuing the trade-off between the two objectives. This enabled the integration of the multi-objective linear optimisation in the two-stage multi-objective optimisation framework.

The optimisation framework was applied to analyse and improve the design of the hybrid solar power plant Atacama-1. The results show that both the financial and technical performance can be optimised. First, it was shown that both, the LCOE and the LPSP of the CSP plant can be improved by its hybridisation with a PV power plant. Whilst the LCOE decreased by 5.6%, the LPSP was reduced by 90%. By varying a single design variable from Atacama-1 it was shown that the energy storage system could be reduced by 33% (from 17.5 to 11.7 h), whereby the LCOE decreases by almost 5% (from 124.6 to 118.78 USD MWh⁻¹), but the LPSP increased from 1.02% to 7.17%. A two-objectives optimisation shows that both the LCOE and investment cost can be reduced simultaneously. However, its reliability was reduced significantly because it was not considered as an objective in the design optimisation.

A three-objective optimisation (LCOE, investment cost and LPSP) was prompted by the increase in LPSP of the previous optimisations. This optimisation shows that both, the technical and financial performance of Atacama-

1 can be simultaneously improved by an optimised design. For example, with an investment of 1443 MUSD (lower than Atacama-1) a decrease in the LCOE from 124.6 to 122.66 USD MWh⁻¹ and a decrease in the LPSP from 1.02% to 0.9% can be reached. Moreover, the optimisation produces a Pareto frontier of non-dominated solutions which show the trade-off between different objectives. Thus the specific design needs to be selected by the developer based on further criteria, such as a limited budget available for the project (investment cost), as well as other environmental or societal performance indicators that could be key for the user of the model.

The large number of potential solutions enabled the development of correlations between the different design parameters (e.g. SM, StH) and objectives (LCOE, investment cost, LPSP) of hybrid solar power plants. These correlations can be used to get a first approximation for the design of hybrid solar power plants. For instance, the reverse correlation between LPSP with LCOE and Investment, indicates the trade-off between technical and financial performance, in addition, the reverse correlation between LPSP with SM and StH suggests that oversized power plants reach better reliability.

This investigation can be applied to any location and for different scenarios: for instance, power plants that supply electricity to the network, as well as off-grid power plants that supply energy to a large end-user company. Besides, the optimisation of the technical and financial performance can be tailored to particular perspectives of the owner of the power plant. In addition, the optimisation framework can be used to evaluate the technical and financial performance of solar power plants as well as the operation of such systems, in order to get key information that supports decision and policy making.

Acknowledgements

Ruben Bravo is supported by a PhD Scholarship from Becas Chile, National Commission for Scientific and Technological Research (CONICYT-Chile).

References

- [1] IEA, Tracking Clean Energy Progress 2017, International Energy Agency, Organisation for Economic Co-operation and Development [doi:10.1787/energy_tech-2014-en](https://doi.org/10.1787/energy_tech-2014-en).
- [2] IEA, Energy Technology Perspectives 2017, International Energy Agency, Organisation for Economic Co-operation and Development [doi:10.1787/energy_tech-2014-en](https://doi.org/10.1787/energy_tech-2014-en).
- [3] P. Denholm, M. Hand, Grid flexibility and storage required to achieve very high penetration of variable renewable electricity, *Energy Policy* 39 (3) (2011) 1817–1830. [doi:10.1016/j.enpol.2011.01.019](https://doi.org/10.1016/j.enpol.2011.01.019).
- [4] P. Denholm, J. Jorgenson, M. Miller, E. Zhou, Methods for Analyzing the Economic Value of Concentrating Solar Power with Thermal Energy Storage, Tech. Rep. July, National Renewable Energy Laboratory (2015).
- [5] IEC, Electrical Energy Storage - White Paper, Tech. rep. (2011). [arXiv:arXiv:1011.1669v3](https://arxiv.org/abs/1011.1669v3), [doi:10.1002/bse.3280020501](https://doi.org/10.1002/bse.3280020501).
- [6] A. Abbas, G. Huff, A. B. Currier, B. C. Kaun, D. M. Rastler, S. B. Chen, D. T. Bradshaw, W. D. Gauntlett, DOE/EPRI 2013 electricity storage handbook in collaboration with NRECA, Tech. Rep. July (2013). [doi:10.1002/SAND2013-5131](https://doi.org/10.1002/SAND2013-5131).
- [7] G. Zini, Energy Storage as a Value Proposition, in: Green Electrical Energy Storage: Science and Finance for Total Fossil Fuel Substitution, McGraw Hill Professional, Access Engineering, 2016.
- [8] NREL, System Advisor Model (SAM) (2011). URL <https://sam.nrel.gov/>
- [9] K. M. Powell, K. Rashid, K. Ellingwood, J. Tuttle, B. D. Iversen, Hybrid concentrated solar thermal power systems: A review, *Renewable and Sustainable Energy Reviews* 80 (2017) 215–237. [doi:10.1016/j.rser.2017.05.067](https://doi.org/10.1016/j.rser.2017.05.067).
- [10] IEA, Technology Roadmap: Solar Thermal Electricity, International Energy Agency, Organisation for Economic Co-operation and Development [doi:10.1007/SpringerReference_7300](https://doi.org/10.1007/SpringerReference_7300).
- [11] NREL, Concentrating Solar Power Projects. URL <https://www.nrel.gov/csp/solarpaces/>
- [12] Solar Reserve LLC, Crescent Dunes (2012). URL <http://www.solarreserve.com/en/global-projects/csp/crescent-dunes>
- [13] I. Rodríguez, C. D. Pérez-Segarra, O. Lehmkuhl, A. Oliva, Modular object-oriented methodology for the resolution of molten salt storage tanks for CSP plants, *Applied Energy* 109 (2013) 402–414. [doi:10.1016/j.apenergy.2012.11.008](https://doi.org/10.1016/j.apenergy.2012.11.008).
- [14] M. Balghouthi, S. E. Trabelsi, M. B. Amara, A. B. H. Ali, A. Guizani, Potential of concentrating solar power (CSP) technology in Tunisia and the possibility of interconnection with Europe, *Renewable and Sustainable Energy Reviews* 56 (2016) 1227–1248. [doi:10.1016/j.rser.2015.12.052](https://doi.org/10.1016/j.rser.2015.12.052).
- [15] C. Parrado, A. Marzo, E. Fuentealba, A. G. Fernandez, 2050 LCOE improvement using new molten salts for thermal energy storage in CSP plants, *Renewable and Sustainable Energy Reviews* 57 (2016) 505–514. [doi:10.1016/j.rser.2015.12.148](https://doi.org/10.1016/j.rser.2015.12.148).
- [16] Abengoa Solar, Abengoa: About Atacama-1 (2016). URL <http://www.abengoa.com/web/en/novedades/atacama-1/acerca/factsheet/>
- [17] M. Petrollese, D. Cocco, Optimal design of a hybrid CSP-PV plant for achieving the full dispatchability of solar energy power plants, *Solar Energy* 137 (2016) 477–489. [doi:10.1016/j.solener.2016.08.027](https://doi.org/10.1016/j.solener.2016.08.027).
- [18] C. A. Pan, F. Dinter, Combination of PV and central receiver CSP plants for base load power generation in South Africa, *Solar Energy* 146 (2017) 379–388. [doi:10.1016/j.solener.2017.02.052](https://doi.org/10.1016/j.solener.2017.02.052).
- [19] G. Srilakshmi, N. Suresh, N. Thirumalai, M. Ramaswamy, Preliminary design of heliostat field and performance analysis of solar tower plants with thermal storage and hybridisation, *Sustainable Energy Technologies and Assessments* 19 (2017) 102–113. [doi:10.1016/j.seta.2016.12.005](https://doi.org/10.1016/j.seta.2016.12.005).
- [20] A. Green, C. Diep, R. Dunn, J. Dent, High Capacity Factor CSP-PV Hybrid Systems, in: *Energy Procedia*, Vol. 69, 2015, pp. 2049–2059. [doi:10.1016/j.egypro.2015.03.218](https://doi.org/10.1016/j.egypro.2015.03.218).
- [21] A. Starke, J. M. Cardemil, R. Escobar, S. Colle, Assessing the performance of hybrid CSP+PV plants in northern Chile, in: *AIP Conference Proceedings*, Vol. 1734, 2016. [doi:10.1063/1.4949230](https://doi.org/10.1063/1.4949230).
- [22] A. S. Wallerand, A. Selviaridis, A. Ashouri, F. Maréchal, Targeting Optimal Design and Operation of Solar Heated Industrial Processes: A MILP Formulation, *Energy Procedia* 91 (91) (2016) 668–680. [doi:10.1016/j.egypro.2016.06.229](https://doi.org/10.1016/j.egypro.2016.06.229).
- [23] S. A. Kalogirou, Optimization of solar systems using artificial neural-networks and genetic algorithms, *Applied Energy* 77 (4) (2004) 383–405. [doi:10.1016/S0306-2619\(03\)00153-3](https://doi.org/10.1016/S0306-2619(03)00153-3).
- [24] O. O. Amusat, P. R. Shearing, E. S. Fraga, Optimal integrated energy systems design incorporating variable renewable energy sources, *Computers & Chemical Engineering* 95 (2016) 21–37. [doi:10.1016/j.compchemeng.2016.08.007](https://doi.org/10.1016/j.compchemeng.2016.08.007).
- [25] Mining Council Chile, Consejo Minero, Reporte Anual 2015, <http://www.consejominero.cl> (2015) 54.
- [26] M. Grageda, M. Escudero, W. Alavia, S. Ushak, V. Fthenakis, Review and multi-criteria assessment of solar energy projects in Chile, *Renewable and Sustainable Energy Reviews* 59 (2016) 583–596. [doi:10.1016/j.rser.2015.12.149](https://doi.org/10.1016/j.rser.2015.12.149).
- [27] G. Cáceres, N. Anrique, A. Girard, J. Degève, J. Baeyens, H. L. Zhang, Performance of molten salt solar power towers in Chile, *Journal of Renewable and Sustainable Energy* 5 (5). [doi:10.1063/1.4826883](https://doi.org/10.1063/1.4826883).
- [28] M. Sengupta, A. Habte, S. Kurtz, A. Dobos, S. Wilbert, E. Lorenz, T. Stoffel, D. Renné, C. Gueymard, D. Myers, S. Wilcox, P. Blanc, R. Perez, Best Practices Handbook for the Collection and Use of Solar Resource Data for Solar Energy Applications, Tech. rep. (2015).
- [29] Ministry of Energy - University of Chile, Explorador Solar Chile - Department of Geophysics (2016). URL <http://www.minenergia.cl/exploradorsolar/>
- [30] D. Y. Goswami, Principles of solar engineering, 3rd Edition, Boca Raton, FL : CRC Press, 2015.
- [31] R. R. Cordero, A. Damiani, G. Seckmeyer, J. Jorquera, M. Caballero, P. Rowe, J. Ferrer, R. Mubarak, J. Carrasco, R. Rondanelli, M. Matus, D. Laroze, The Solar Spectrum in the Atacama Desert, *Scientific Reports* 6 (2016) 22457. [doi:10.1038/srep22457](https://doi.org/10.1038/srep22457).
- [32] S. Northey, N. Haque, G. Mudd, Using sustainability reporting to assess the environmental footprint of copper mining, *Journal of Cleaner Production* 40 (2013) 118–128. [doi:10.1016/j.jclepro.2012.09.027](https://doi.org/10.1016/j.jclepro.2012.09.027).
- [33] Comisión Chilena del Cobre, Yearbook: Copper and other Mineral Statistics 1996-2015, Tech. rep. (2016).
- [34] CDEC-SING, Annual Report and Operational Statistics 2015, Tech. rep. (2015).
- [35] Ministry of Energy - Chilean Government, Indicadores Ambientales del Sector Energía. URL <http://www.minenergia.cl/indicadoresambientales/>
- [36] Servicio de Evaluación Ambiental, Sistema de Evaluación de Impacto Ambiental e-seia (2014). URL <http://seia.sea.gob.cl>
- [37] J. Houston, Variability of precipitation in the Atacama Desert: Its causes and hydrological impact, *International Journal of Climatology* 26 (15) (2006) 2181–2198. [arXiv:joc.1492](https://arxiv.org/abs/joc.1492), [doi:10.1002/joc.1359](https://doi.org/10.1002/joc.1359).
- [38] IEA, NEA, OECD, Projected Costs of Generating Electricity 2015, International Energy Agency, Nuclear Energy Agency, Organisation for Economic Co-operation and Development [arXiv:arXiv:1011.1669v3](https://arxiv.org/abs/1011.1669v3), [doi:10.1787/cost_electricity-2015-en](https://doi.org/10.1787/cost_electricity-2015-en).
- [39] B. H. Gebreslassie, G. Guillén Gosálbez, L. Jiménez, D. Boer, Design of environmentally conscious absorption cooling systems via multi-objective optimization and life cycle assessment, *Applied Energy* 86 (9) (2009) 1712–1722. [doi:10.1016/j.apenergy.2008.11.019](https://doi.org/10.1016/j.apenergy.2008.11.019).
- [40] A.-T. Nguyen, S. Reiter, P. Rigo, A review on simulation-based optimization methods applied to building performance analysis, *Applied Energy* 113 (2014) 1043–1058. [doi:10.1016/j.apenergy.2013.08.061](https://doi.org/10.1016/j.apenergy.2013.08.061).

- [41] S. Fazlollahi, P. Mandel, G. Becker, F. Maréchal, Methods for multi-objective investment and operating optimization of complex energy systems, *Energy* 45 (1) (2012) 12–22. doi: 10.1016/j.energy.2012.02.046.